CHAPTER

8

CONTROLLED-CURRENT TECHNIQUES

8.1 INTRODUCTION

We discussed in Chapters 5–7 methods in which the potential of an electrode was controlled (or was the independent variable), while the current (the dependent variable) was determined as a function of time. In this chapter we consider the opposite case, where the current is controlled (frequently held constant), and the potential becomes the dependent variable, which is determined as a function of time. The other conditions assumed in Chapters 5–7, such as small ratio of electrode area to solution volume and semi-infinite diffusion, are also assumed here. We do not treat UMEs, because the behavior in the steady-state regime is not a function of whether the applied signal is a controlled potential or current. The experiment is carried out by applying the controlled current between the working and auxiliary electrodes with a current source (called a *galvanostat*) and recording the potential between the working and reference electrodes (e.g., with a recorder, oscilloscope, or other data acquisition device) (Figure 8.1.1). These techniques are generally called *chronopotentiometric* techniques, because E is determined as a function of time, or *galvanostatic* techniques, because a small constant current is applied to the working electrode.

8.1.1 Comparison with Controlled-Potential Methods

Since the general aspects of controlled-potential and controlled-current experiments are so similar, we might consider the basic differences between the two types of experiments and the relative advantages of each. The instrumentation for controlled-current experiments is simpler than the potentiostats required in controlled-potential ones, since no feedback from the reference electrode to the control device is required. Although constant-current sources constructed from operational amplifiers are frequently used, a simple circuit employing a high-voltage power supply (e.g., a 400-V power supply or several 90-V batteries) and a large resistor can be adequate. The mathematical treatment also differs from what we have already seen. In controlled-current exper-

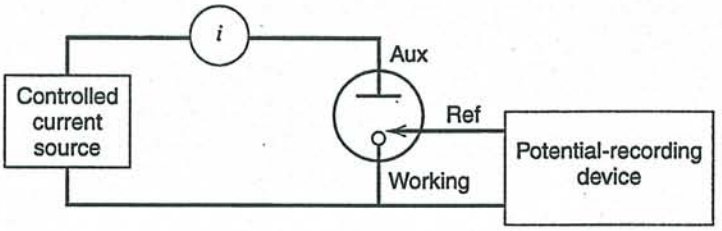

Figure 8.1.1 Simplified block diagram of apparatus for chronopotentiometric measurements.

iments, the surface boundary condition is based on the known current or fluxes (i.e., the concentration gradients) at the electrode surface, while in controlled-potential methods, the concentrations at $x = 0$ (as functions of E) provide the boundary conditions. Usually the mathematics involved in solving the diffusion equations in controlled-current problems are much simpler, and closed-form analytical solutions are usually obtained.

A fundamental disadvantage of controlled-current techniques is that double-layer charging effects are frequently larger and occur throughout the experiment in such a way that correction for them is not straightforward. Treating data from multicomponent systems and stepwise reactions is also more complicated in controlled-current methods, and the waves observed in E-t transients are usually less well-defined than those of potential sweep i-E curves.

Controlled-current methods can be of particular value when the process being studied is the background process, such as solvated electron formation in liquid ammonia or reduction of quaternary ammonium ion in an aprotic solvent. A simple method for determination of the thickness of metal films is by anodic stripping at constant current. Working with background processes in a controlled-potential mode is often difficult.

8.1.2 Classification and Qualitative Description

Different types of constant-current techniques are illustrated in Figure 8.1.2. Let us first consider *constant-current chronopotentiometry* (Figure 8.1.2*a*) in the context of the anthracene (An) system used as an example in Section 5.1.1. The steady current, i, applied to the electrode causes the anthracene to be reduced at a constant rate to the anion radical, $An^{\cdot-}$. The potential of the electrode moves to values characteristic of the couple and varies with time as the $An/An^{\cdot-}$ concentration ratio changes at the electrode surface. The process can be regarded as a titration of the An in the vicinity of the electrode by the continuous flux of electrons, resulting in an E-t curve like that obtained for a potentiometric titration (E as a function of titrant added, $i \cdot t$). Eventually, after the concentration of An drops to zero at the electrode surface, the flux of An to the surface is insufficient to accept all of the electrons being forced across the electrode-solution interface. The potential of the electrode will then rapidly shift toward more negative values until a new, second reduction process can start. The time after application of the constant current when this potential transition occurs is called the *transition time*, τ. It is related to the concentration and the diffusion coefficient and is the chronopotentiometric analogue of the peak or limiting current in controlled-potential experiments. The shape and location of the E-t curve is governed by the reversibility, or the heterogeneous rate constant, of the electrode reaction.

Instead of a constant current, one can apply a current that varies as a known function of time (e.g., $i = \beta t$, a current ramp; Figure 8.1.2*b*). Although this technique, called *programmed current chronopotentiometry*, can be treated theoretically with little difficulty, it has been employed infrequently. The current can also be reversed after some time (*current reversal chronopotentiometry*, Figure 8.1.2*c*). For example, if in the case considered above, the current is suddenly changed to an anodic current of equal magnitude at, or before, the transition time, the $An^{\cdot-}$ formed during the forward step will start oxidizing. The potential will move in a positive direction as the $An/An^{\cdot-}$ concentration ratio increases. When the $An^{\cdot-}$ concentration falls to zero at the electrode surface, a potential transition toward positive potentials occurs, and a reverse transition time can be measured. In an extension of this technique the current can be continuously reversed at each transition, resulting in *cyclic chronopotentiometry* (Figure 8.1.2*d*). Finally, as in the treatment of

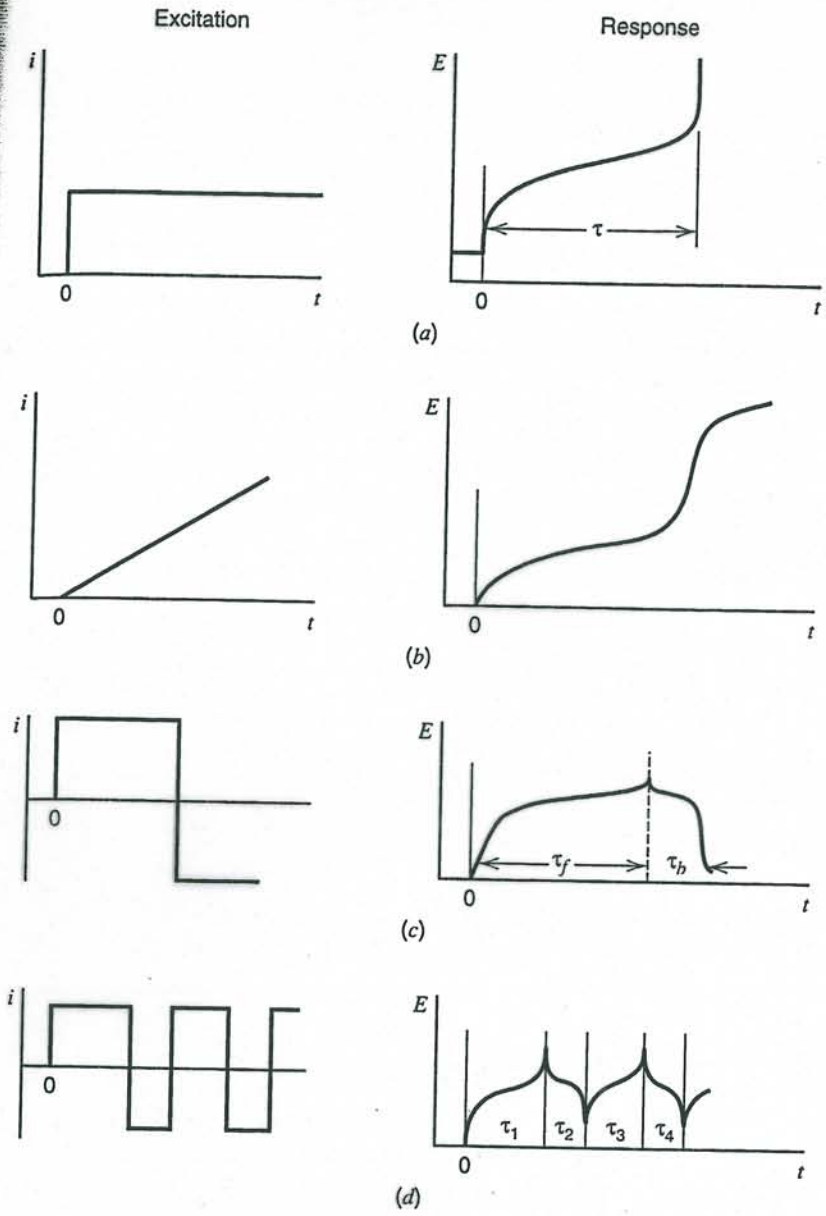

Figure 8.1.2 Different types of controlled-current techniques. (*a*) Constant-current chronopotentiometry. (*b*) Chronopotentiometry with linearly increasing current. (*c*) Current reversal chronopotentiometry. (*d*) Cyclic chronopotentiometry.

controlled-potential data, the derivatives of the *E*-*t* curves can be obtained or differential methods can be employed.[1]

8.2 GENERAL THEORY OF CONTROLLED-CURRENT METHODS

8.2.1 Mathematics of Semi-Infinite Linear Diffusion

We again consider the simple electron-transfer reaction, $O + ne \rightarrow R$. A planar working electrode and an unstirred solution are assumed, with only species O initially present at a concentration C_O^*. These conditions are the same as those in Section 5.4.1, so that the diffusion equations and general boundary conditions, (5.4.2) to (5.4.5), apply:

$$\frac{\partial C_O(x,t)}{\partial t} = D_O\left[\frac{\partial^2 C_O(x,t)}{\partial x^2}\right] \tag{8.2.1}$$

[1]These latter methods are employed infrequently and are discussed in more depth in the first edition, Sections 7.4.3 and 7.6.

$$\frac{\partial C_R(x,t)}{\partial t} = D_R\left[\frac{\partial^2 C_R(x,t)}{\partial x^2}\right] \tag{8.2.2}$$

$$\left.\begin{array}{c}\text{At } t = 0 \text{ (for all } x)\\ \text{and}\\ \text{as } x \to \infty \text{ (for all } t)\end{array}\right\} C_O(x,t) = C_O^* \qquad C_R(x,t) = 0 \tag{8.2.3}$$

$$D_O\left[\frac{\partial C_O(x,t)}{\partial x}\right]_{x=0} + D_R\left[\frac{\partial C_R(x,t)}{\partial x}\right]_{x=0} = 0 \tag{8.2.4}$$

Since the applied current $i(t)$ is presumed known, the flux at the electrode surface is also known at any time, by the equation [see (4.4.29)]:

Constant flux boundary condition

$$D_O\left[\frac{\partial C_O(x,t)}{\partial x}\right]_{x=0} = \frac{i(t)}{nFA} = -J_O(0,t) \tag{8.2.5}$$

This boundary condition involving the concentration *gradient* allows the diffusion problem to be solved without reference to the rate of the electron-transfer reaction, in contrast with the concentration-potential boundary conditions required for controlled-potential methods. Although in many controlled-current experiments the applied current is constant, the more general case for any arbitrarily applied current, $i(t)$, can be solved readily and includes the constant-current case, as well as reversal experiments and several others of interest.

For species O, application of the Laplace transform method to (8.2.1) and (8.2.3) yields

$$\bar{C}_O(x,s) = \frac{C_O^*}{s} + A(s)\exp\left[-\left(\frac{s}{D_O}\right)^{1/2} x\right] \tag{8.2.6}$$

The transform of (8.2.5) is

$$D_O\left[\frac{\partial \bar{C}_O(x,s)}{\partial x}\right]_{x=0} = \frac{\bar{i}(s)}{nFA} \tag{8.2.7}$$

By taking the indicated derivative of (8.2.6) and substituting in (8.2.7) to eliminate $A(s)$, we have

$$\bar{C}_O(x,s) = \frac{C_O^*}{s} - \left[\frac{\bar{i}(s)}{nFAD_O^{1/2}s^{1/2}}\right]\exp\left[-\left(\frac{s}{D_O}\right)^{1/2} x\right] \tag{8.2.8}$$

By substitution of the known function, $\bar{i}(s)$, and employing the inverse transform, $C_O(x,t)$ can be obtained. Similarly, the following expression for $\bar{C}_R(x,s)$ can be derived:

$$\bar{C}_R(x,s) = \left[\frac{\bar{i}(s)}{nFAD_R^{1/2}s^{1/2}}\right]\exp\left[-\left(\frac{s}{D_R}\right)^{1/2} x\right] \tag{8.2.9}$$

Note that direct inversion of (8.2.8) and (8.2.9) using the convolution property leads to (6.2.8) and (6.2.9). These integral forms are also convenient for solving controlled-current problems.

8.2.2 Constant-Current Electrolysis—The Sand Equation

If $i(t)$ is constant, then $\bar{i}(s) = i/s$ and (8.2.8) becomes

$$\bar{C}_O(x,s) = \frac{C_O^*}{s} - \left[\frac{i}{nFAD_O^{1/2}s^{3/2}}\right]\exp\left[-\left(\frac{s}{D_O}\right)^{1/2} x\right] \tag{8.2.10}$$

The inverse transform of this equation yields the expression for $C_O(x, t)$:

$$C_O(x, t) = C_O^* - \frac{i}{nFAD_O}\left\{2\left(\frac{D_O t}{\pi}\right)^{1/2} \exp\left(-\frac{x^2}{4D_O t}\right) - x\,\mathrm{erfc}\left[\frac{x}{2(D_O t)^{1/2}}\right]\right\} \quad (8.2.11)$$

Typical concentration profiles at various times during a constant-current electrolysis are given in Figure 8.2.1. Note that $C_O(0, t)$ decreases continuously, yet $[\partial C_O(x, t)/\partial x]_{x=0}$ is constant at all times after the onset of electrolysis.

An expression for $C_O(0, t)$ can be obtained by setting $x = 0$ in (8.2.11), or directly by inverse transform of (8.2.8) with $x = 0$:

$$\bar{C}_O(0, s) = \frac{C_O^*}{s} - \frac{i}{nFAD_O^{1/2}s^{3/2}} \quad (8.2.12)$$

to yield

$$C_O(0, t) = C_O^* - \frac{2it^{1/2}}{nFAD_O^{1/2}\pi^{1/2}} \quad (8.2.13)$$

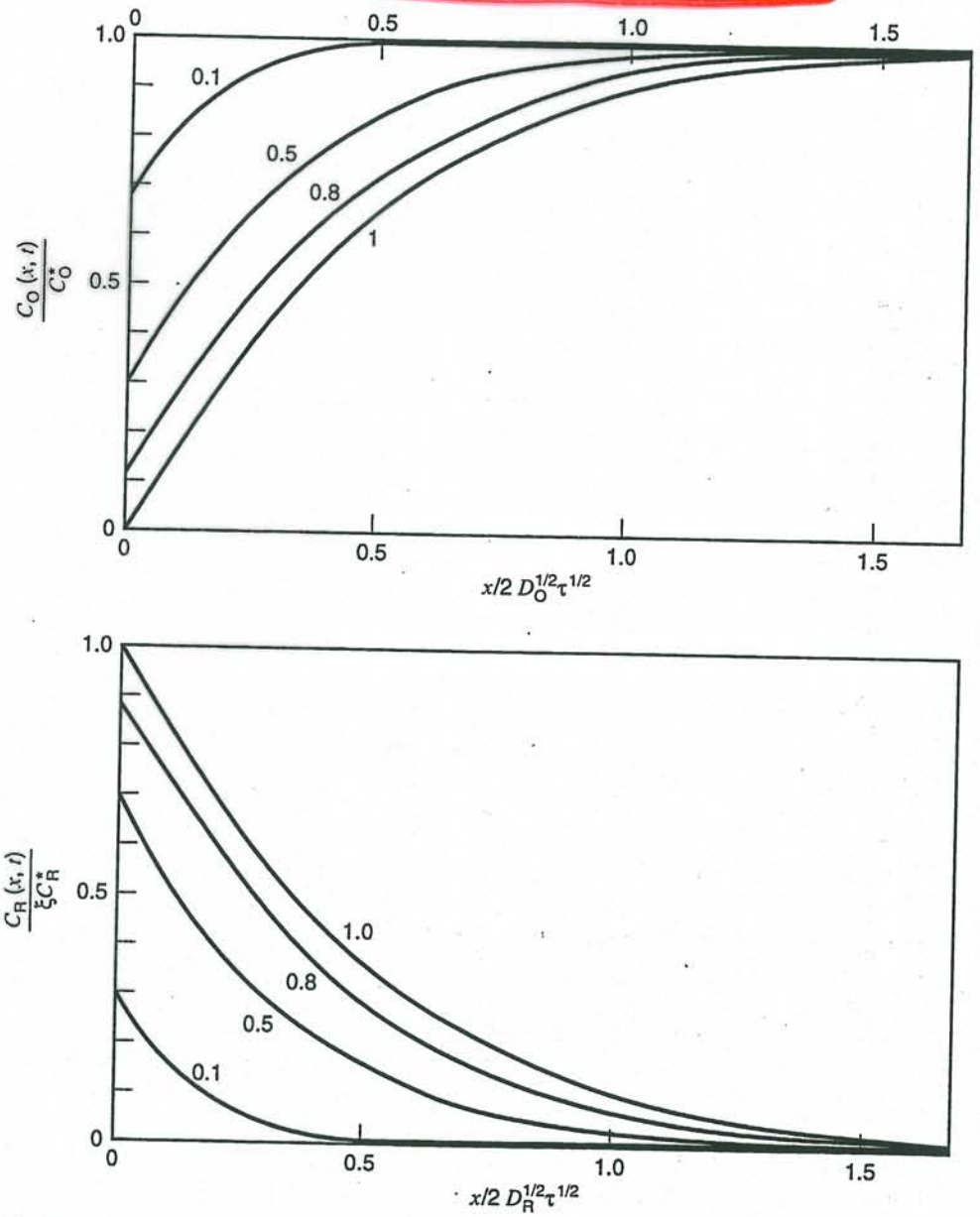

Figure 8.2.1 Concentration profiles of O and R (in dimensionless form) at various values of t/τ indicated on the curves.

At the transition time, τ, $C_O(0, t)$ drops to zero and (8.2.13) becomes

$$\frac{i\tau^{1/2}}{C_O^*} = \frac{nFAD_O^{1/2}\pi^{1/2}}{2} = 85.5nD_O^{1/2}A\,\frac{\text{mA-s}^{1/2}}{\text{m}M}\ (\text{with } A \text{ in cm}^2) \tag{8.2.14}$$

This equation, known as the *Sand equation*, was first derived by H. J. S. Sand (1).

As discussed in Section 8.1.2, the flux of O to the electrode surface beyond the transition time is not large enough to satisfy the applied current, and the potential shifts to a more extreme value where another electrode process can occur (Figure 8.2.2). The actual shape of the E-t curve is discussed in the next sections.

The measured value of τ at known i (or better, the values of $i\tau^{1/2}$ obtained at various currents) can be used to determine n, A, C_O^* or D_O. For a well-behaved system, the *transition time constant*, $i\tau^{1/2}/C_O^*$, is independent of i or C_O^*. A lack of constancy in this parameter indicates complications to the electrode reaction from coupled homogeneous chemical reactions (Chapter 12), adsorption (Chapter 14), or measurement artifacts, such as double-layer charging or the onset of convection (Section 8.3.5).

Note that (8.2.11) can be written in a convenient form with dimensionless groupings $C_O(x, t)/C_O^*$, t/τ, and $\chi_O = x/[2(D_O t)^{1/2}]$ for $(0 \le t \le \tau)$:

$$\frac{C_O(x, t)}{C_O^*} = 1 - \left(\frac{t}{\tau}\right)^{1/2}[\exp(-\chi_O^2) - \pi^{1/2}\chi_O\,\text{erfc}(\chi_O)] \tag{8.2.15}$$

$$\frac{C_O(0, t)}{C_O^*} = 1 - \left(\frac{t}{\tau}\right)^{1/2} \tag{8.2.16}$$

In a similar way, the following equations hold for $C_R(x, t)$ when $(0 \le t \le \tau)$:

$$\frac{C_R(x, t)}{C_R^*} = \xi\left(\frac{t}{\tau}\right)^{1/2}[\exp(\chi_R^2) - \pi^{1/2}\chi_R\,\text{erfc}(\chi_R)] \tag{8.2.17}$$

where $\chi_R = x/[2(D_R t)^{1/2}]$ and $\xi = (D_O/D_R)^{1/2}$. Accordingly,

$$C_R(0, t) = \frac{2it^{1/2}}{nFA\pi^{1/2}D_R^{1/2}} = \xi\left(\frac{t}{\tau}\right)^{1/2}C_O^* \tag{8.2.18}$$

See Figure 8.2.1.

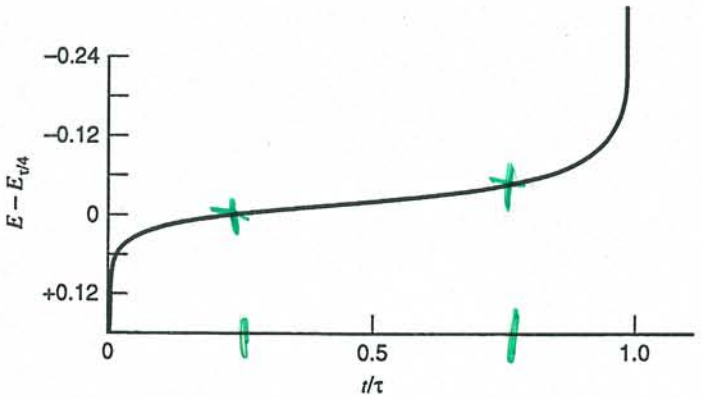

Figure 8.2.2 Theoretical chronopotentiogram for a nernstian electrode process.

8.2.3 Programmed Current Chronopotentiometry

It is possible to use currents that are programmed to vary with time in a special way, rather than remaining constant (2, 3). For example, a current that increases linearly with time could be used:

$$i(t) = \beta t \qquad (8.2.19)$$

The treatment follows that for a constant-current electrolysis. In this case the transform is

$$\bar{i}(s) = \frac{\beta}{s^2} \qquad (8.2.20)$$

so that (8.2.8) becomes, at $x = 0$,

$$\bar{C}_O(0, s) = \frac{C_O^*}{s} - \frac{\beta}{nFAD_O^{1/2}s^{5/2}} \qquad (8.2.21)$$

$$C_O(0, t) = C_O^* - \frac{2\beta t^{3/2}}{nFAD_O^{1/2}\Gamma(5/2)} \qquad (8.2.22)$$

where $\Gamma(5/2)$ is the mathematical gamma function, equal with this argument to 1.33. This same treatment can be employed with any power function of time.

A particularly interesting applied current is one varying with the square root of time:

$$i(t) = \beta t^{1/2} \qquad (8.2.23)$$

$$\bar{i}(s) = \frac{\beta\pi^{1/2}}{2s^{3/2}} \qquad (8.2.24)$$

$$\bar{C}_O(0, s) = \frac{C_O^*}{s} - \frac{\beta\pi^{1/2}}{2nFAD_O^{1/2}s^2} \qquad (8.2.25)$$

$$C_O(0, t) = C_O^* - \frac{\beta\pi^{1/2}t}{2nFAD_O^{1/2}} \qquad (8.2.26)$$

Again, defining the transition time τ as that time when $C_O(0, t) = 0$, an expression equivalent to the constant-current Sand equation results, but with τ (rather than $\tau^{1/2}$) proportional to C_O^* and β:

$$\frac{\beta\tau}{C_O^*} = 2nFA\pi^{-1/2}D_O^{1/2} \qquad (8.2.27)$$

Because this current excitation function is fairly difficult to generate, the technique has not been used very much. Nevertheless, it would be advantageous for stepwise electron-transfer reactions and multicomponent systems (see Section 8.5).

8.3 POTENTIAL–TIME CURVES IN CONSTANT-CURRENT ELECTROLYSIS

8.3.1 Reversible (Nernstian) Waves

For rapid electron transfer, a nernstian relationship links the potential with the surface concentrations of O and R (Sections 3.4.5 and 3.5.3). Substitution of the expressions for $C_O(0, t)$ and $C_R(0, t)$, equations 8.2.16 and 8.2.18, into (3.5.21) yields (4)

$$E = E_{\tau/4} + \frac{RT}{nF}\ln\frac{\tau^{1/2} - t^{1/2}}{t^{1/2}} \qquad (8.3.1)$$

where $E_{\tau/4}$, the *quarter-wave potential*, is

$$E_{\tau/4} = E^{0'} - \frac{RT}{2nF} \ln \frac{D_O}{D_R} \tag{8.3.2}$$

Thus $E_{\tau/4}$ is the chronopotentiometric equivalent of the voltammetric $E_{1/2}$ value (Figure 8.2.2). The test for reversibility of an E-t curve is a linear plot of E *vs.* $\log [(\tau^{1/2} - t^{1/2})/t^{1/2}]$ having a slope of $59/n$ mV, or a value of $|E_{\tau/4} - E_{3\tau/4}| = 47.9/n$ mV (at 25°C).

8.3.2 Totally Irreversible Waves

For a totally irreversible one-step, one electron reaction

$$O + e \xrightarrow{k_f} R \tag{8.3.3}$$

the current is related to the potential by either of the following equations (5):

$$i = nFAk_f^0 C_O(0, t) \exp\left[\frac{-\alpha F E}{RT}\right] \tag{8.3.4a}$$

$$i = nFAk^0 C_O(0, t) \exp\left[\frac{-\alpha F (E - E^{0'})}{RT}\right] \tag{8.3.4b}$$

When the expression for $C_O(0, t)$, (8.2.16), is substituted into these equations, the following expressions result:

$$E = \frac{RT}{\alpha F} \ln\left(\frac{FAC_O^* k_f^0}{i}\right) + \frac{RT}{\alpha F} \ln\left[1 - \left(\frac{t}{\tau}\right)^{1/2}\right] \tag{8.3.5a}$$

$$E = E^{0'} + \frac{RT}{\alpha F} \ln\left(\frac{FAC_O^* k^0}{i}\right) + \frac{RT}{\alpha F} \ln\left[1 - \left(\frac{t}{\tau}\right)^{1/2}\right] \tag{8.3.5b}$$

Equivalent expressions can be obtained by using the Sand equation and substituting for $\tau^{1/2}$:

$$E = \frac{RT}{\alpha F} \ln\left[\frac{2k_f^0}{(\pi D_O)^{1/2}}\right] + \frac{RT}{\alpha F} \ln[\tau^{1/2} - t^{1/2}] \tag{8.3.6a}$$

$$E = E^{0'} + \frac{RT}{\alpha F} \ln\left[\frac{2k^0}{(\pi D_O)^{1/2}}\right] + \frac{RT}{\alpha F} \ln[\tau^{1/2} - t^{1/2}] \tag{8.3.6b}$$

Thus, for a totally irreversible reduction wave, the whole E-t wave shifts toward more negative potentials with increasing current, with a tenfold increase in current causing a shift of $2.3RT/\alpha F$ (or $59/\alpha$ mV at 25°C). Note that uncompensated resistance between the reference and working electrodes will also cause the E-t curve to shift with increasing i. For a totally irreversible wave, $|E_{\tau/4} - E_{3\tau/4}| = 33.8/\alpha$ mV at 25°C.

8.3.3 Quasireversible Waves

For the quasireversible one-step, one-electron process,

$$O + e \underset{k_b}{\overset{k_f}{\rightleftarrows}} R \tag{8.3.7}$$

a general E-t relationship is found from combining the current-overpotential equation, (3.4.10), with the equations for $C_O(0, t)$, (8.2.16), and $C_R(0, t)$, (8.2.18). A bulk concen-

tration of R, C_R^*, is required, so that a starting equilibrium potential can be defined (6, 7). This requirement adds the term C_R^* to (8.2.18). The overall result is

$$\frac{i}{i_0} = \left[1 - \frac{2i}{FAC_O^*}\left(\frac{t}{\pi D_O}\right)^{1/2}\right]e^{-\alpha f\eta} - \left[1 + \frac{2i}{FAC_R^*}\left(\frac{t}{\pi D_R}\right)^{1/2}\right]e^{(1-\alpha)f\eta} \tag{8.3.8}$$

Alternative forms can be written in terms of the current density, j, and the heterogeneous rate constants,

$$j = k_f\left[FC_O^* - 2j\left(\frac{t}{\pi D_O}\right)^{1/2}\right] - k_b\left[FC_R^* + 2j\left(\frac{t}{\pi D_R}\right)^{1/2}\right] \tag{8.3.9a}$$

or, when $C_R^* = 0$,

$$j = Fk_fC_O^* - \frac{2jt^{1/2}}{\pi^{1/2}}\left(\frac{k_f}{D_O^{1/2}} + \frac{k_b}{D_R^{1/2}}\right) \tag{8.3.9b}$$

where k_f and k_b are defined in (3.3.9) and (3.3.10).

Usually, the study of the kinetics of quasireversible electrode reactions by constant-current techniques (generally called the *galvanostatic or current step* method) involves small current perturbations, and the potential change from the equilibrium position is also small. When both O and R are initially present, the linearized current-potential-concentration characteristic, (3.5.33), can be employed. Combination with equations 8.2.13 and 8.2.18 (with the latter modified by an added term, C_R^*) yields

$$-\eta = \frac{RT}{F}i\left[\frac{2t^{1/2}}{FA\pi^{1/2}}\left(\frac{1}{C_O^*D_O^{1/2}} + \frac{1}{C_R^*D_R^{1/2}}\right) + \frac{1}{i_0}\right] \tag{8.3.10}$$

The same result can be obtained by linearization of (8.3.8). Thus, a plot of η *vs.* $t^{1/2}$, for small values of η, will be linear, and i_0 can be obtained from the intercept. This method is the constant-current analog of the potential step method discussed in Section 5.5.1(c).

8.3.4 General Effects of Double-Layer Capacity

Because the potential is changing during the application of the current step, there is always a nonfaradaic current that contributes to charging of the double-layer capacitance. If $dA/dt = 0$, then i_c is given by

$$i_c = -AC_d(d\eta/dt) = -AC_d(dE/dt) \tag{8.3.11}$$

Thus, of the total applied constant current, i, only a portion, i_f, goes to the faradaic reaction:

$$i_f = i - i_c \tag{8.3.12}$$

Since dE/dt is a function of time, i_c and i_f also vary with time, even when i is constant. This situation can be treated as a case of programmed current chronopotentiometry if an explicit form of dE/dt or $d\eta/dt$ is known.

For the case where the one-step, one-electron process applies and the general η-t expression can be linearized, then (8.3.10) can be adapted as follows (8):

$$-\eta = \frac{RT}{F}i\left[\frac{2t^{1/2}}{\pi^{1/2}}N - \frac{RT}{F}AC_dN^2 + \frac{1}{i_0}\right] \tag{8.3.13}$$

where

$$N = \frac{1}{FA}\left(\frac{1}{C_O^* D_O^{1/2}} + \frac{1}{C_R^* D_R^{1/2}}\right) \tag{8.3.14}$$

The intercept of the η-$t^{1/2}$ plot allows the determination of $1/i_0$ only when this term is appreciable compared to $(RT/F)AC_dN^2$ (8). To overcome this limitation for fast electron-transfer reactions, where i_0 is large, the galvanostatic double-pulse method has been proposed (Section 8.6).

8.3.5 Practical Issues in the Measurement of Transition Time

As discussed in Section 8.3.4, the presence of a finite double-layer capacity results in a charging current contribution proportional to dE/dt (equation 8.3.11) and causes i_f to differ from the total applied current, i. This effect, which is largest immediately after application of the current and near the transition (where dE/dt is relatively large), affects the overall shape of the E-t curve and makes measurement of τ difficult and inaccurate. A number of authors have examined this problem and have proposed techniques for measuring τ from distorted E-t curves or for correcting values obtained in the presence of significant double-layer effects.

In the simplest approach, i_c is assumed to be constant for $0 < t < \tau$. This is not strictly so, of course, since dE/dt and C_d (a function of E) change throughout the E-t curve (9, 10); however the approximation leads to

$$i = i_f + i_c \tag{8.3.15}$$

$$\frac{i\tau^{1/2}}{C_O^*} = \frac{i_f\tau^{1/2}}{C_O^*} + \frac{i_c\tau}{C_O^*\tau^{1/2}} \tag{8.3.16}$$

where $i_f\tau^{1/2}/C_O^*$ is the "true" chronopotentiometric constant, a, equal to $nFAD_O^{1/2}\pi^{1/2}/2$. In the last term, $i_c\tau$ is the total number of coulombs needed to charge an average double-layer capacitance from the initial potential to the potential at which τ is measured (ΔE), so that $i_c\tau \approx (C_d)_{avg}\,\Delta E$, and is represented by a correction factor b. Thus the final equation is

$$i\tau^{1/2}/C_O^* = a + b/C_O^*\tau^{1/2} \tag{8.3.17}$$

Plots based on (8.3.17) can thus be used to extract a and b from the observed data (e.g., a plot of $i\tau$ *vs.* $\tau^{1/2}$ yields a slope aC_O^* and an intercept b).

An equation of this form can also be used to correct for formation of an oxide film (e.g., on a platinum electrode during an electrochemical oxidation) and for electrolysis of adsorbed material in addition to diffusing species. Under these conditions, (8.3.15) becomes (10):

$$i = i_f + i_c + i_{ox} + i_{ads} \tag{8.3.18}$$

where i_{ox} is the current going to formation (or reduction) of the oxide film and i_{ads} is the current required for the adsorbed material. A treatment similar to that given above again yields (8.3.17), where b is now an overall correction factor including $Q_{ox} = i_{ox}\tau$ and $Q_{ads} = nF\Gamma$, where Γ is the number of moles of adsorbed species per square centimeter (Section 14.3.7). Although these approximations are rough, treatments of actual experimental data by (8.3.17) yield fairly good results, even at rather low concentrations and short transition times, where these surface effects are most important (11).

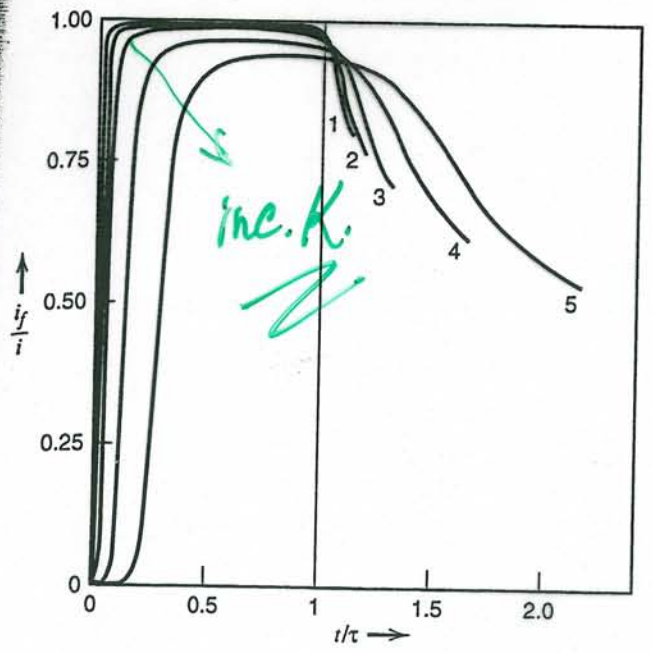

Figure 8.3.1 Fraction of total current contributing to the faradaic process (i_f/i) *vs.* time for a nernstian electrode process. K values of (*1*) 5×10^{-4}; (*2*) 10^{-3}; (*3*) 2×10^{-3}; (*4*) 5×10^{-3}; (5) 0.01. [From W. T. de Vries, *J. Electroanal. Chem.*, **17**, 31 (1968), with permission.]

A more rigorous approach involves only the assumption that C_d is independent of E (12–14). In this case, one must solve the diffusion equation, (8.2.1), beginning with the usual boundary conditions, (8.2.3). The flux condition, (8.2.5), is replaced by

$$i = nFAD_O\left(\frac{\partial C_O}{\partial x}\right)_{x=0} + AC_d\left(\frac{dE}{dt}\right) \tag{8.3.19}$$

In addition, one needs the appropriate i-E characteristic (i.e., for a reversible, totally irreversible, or quasireversible reaction). The resulting nonlinear integral equation must be evaluated numerically. Alternatively, the problem can be addressed by digital simulation techniques. Figures 8.3.1 and 8.3.2 illuminate the effects of different relative contributions of double-layer charging on i_f (at constant i) and on the E-t curves of a nernstian reaction. The charging contribution is represented there by the dimensionless parameter, K, defined as

$$K = \left(\frac{RT}{nF}\right)\frac{C_d}{nFC_O^*(\pi D_O\tau)^{1/2}} \tag{8.3.20}$$

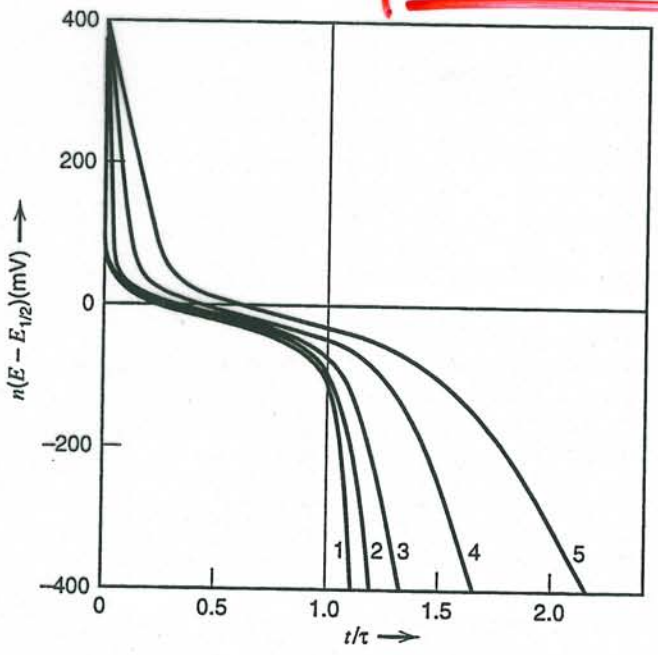

Figure 8.3.2 Effect of double-layer capacitance on chronopotentiograms for a nernstian electrode reaction. Values of K as in Figure 8.3.1. [From W. T. de Vries, *J. Electroanal. Chem.*, **17**, 31 (1968), with permission.]

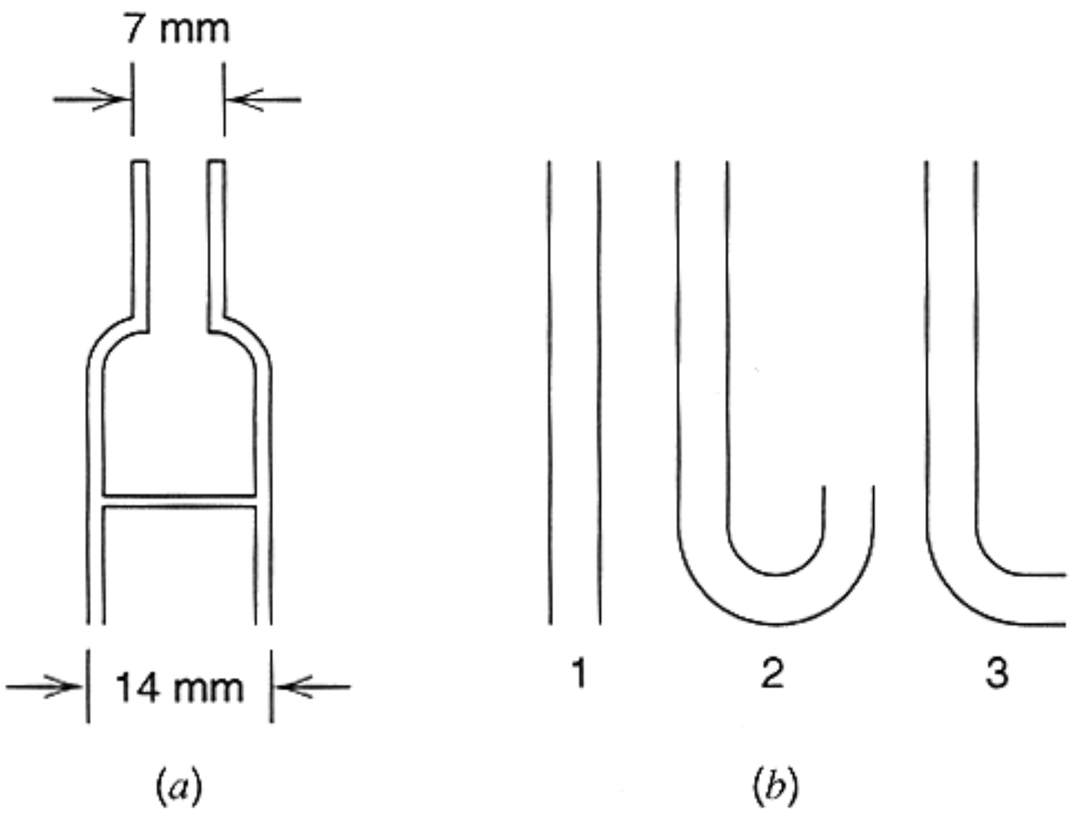

Figure 8.3.3 (*a*) Shielded electrode for maintaining linear diffusion and suppressing convection. (*b*) Tubes to which shielded electrode is attached to provide: (*1*) horizontal electrode, diffusion upward; (*2*) horizontal electrode, diffusion downward; (*3*) vertical electrode. [Reprinted with permission from A. J. Bard, *Anal. Chem.*, **33**, 11 (1961). Copyright 1961, American Chemical Society.]

The effect of double-layer charging is clearly most important at small τ values (see equation 8.3.20). Problems with distorted *E-t* curves and the difficulty of obtaining corrected τ values have discouraged the use of controlled-current methods as opposed to controlled-potential ones.

In both controlled-current and controlled-potential methods, problems develop at long experimental times because of the onset of convection and the nonlinearity of diffusion. Convective effects, caused by motion of the solution with respect to the electrode, can arise by accidental vibrations transmitted to the cell (e.g., by hood fans, vacuum pumps, passing traffic) or as a result of density gradients building up at the electrode surface because of differences in density between reactants and products (so-called "natural convection"). Convective effects can be minimized by using electrodes with glass mantles (shielded electrodes; Figure 8.3.3) and by orienting the electrode horizontally so that the denser species is always below the less dense one (15, 16). Vertically oriented electrodes (e.g., foils or wires) often suffer from convection effects even at not very long times (e.g., 60 to 80 s). The shielded electrode also has the virtue of constraining diffusion to lines normal to the electrode surface so that true linear diffusion conditions are approached. An unshielded electrode, such as a platinum disk imbedded in glass can show appreciable "sphericity" effects when the diffusion layer thickness is not negligible with respect to the electrode dimensions; that is, material can diffuse to the unshielded electrode from the sides. This effect causes increases in the transition time (or anomalously large currents in controlled-potential methods). With properly oriented shielded electrodes, however, linear diffusion conditions can be maintained for 300 s or longer.

▶ 8.4 REVERSAL TECHNIQUES

8.4.1 Response Function Principle

A useful technique for treating reversal methods in chronopotentiometry (and other techniques in electrochemistry) is based on the *response function principle* (2, 17). This method, which is also used to treat electrical circuits, considers the system's response to a perturbation or excitation signal, as applied in Laplace transform space. One can write the general equation (2)

$$\bar{R}(s) = \bar{\Psi}(s)\bar{S}(s) \tag{8.4.1}$$

where $\bar{\Psi}(s)$ is the excitation function transform, $\bar{R}(s)$ is the response transform, which describes how the system responds to the excitation, and $\bar{S}(s)$ is the system transform, which

7.6 DERIVATIVE METHODS

By rather straightforward instrumental approaches the derivative of the chronopotentiogram, that is, a curve of dE/dt *vs.* t, can be obtained. The theoretical form of the derivative curve can readily be found by differentiation of the appropriate E-t expression. Thus for a nernstian process, from (7.3.1),

$$\frac{dE}{dt} = -\left(\frac{RT}{2nF}\right)\left[\frac{\tau^{1/2}}{t(\tau^{1/2} - t^{1/2})}\right] \tag{7.6.1}$$

While finding τ from the maximum of the derivative curve is possible, its determination by this approach suffers the same problems as the direct measurement approach. As an alternative, Peters and Burden (29) recommended that the minimum in the derivative curve, which for a nernstian process occurs at $t = 4\tau/9$, be evaluated. Since

$$(dE/dt)_{\text{min,rev}} = -(27/8)\left(\frac{RT}{nF\tau}\right) \tag{7.6.2}$$

$$= -0.08664/n\tau \text{ V sec}^{-1} \text{ at } 25\ ^\circ\text{C} \tag{7.6.3}$$

τ can be obtained by a direct evaluation of $(dE/dt)_{\text{min}}$. Typical experimental results are shown in Figure 7.6.1.

For a totally irreversible reaction, (see equation 7.3.6),

$$\frac{dE}{dt} = -\left(\frac{RT}{2\alpha n_a F}\right)[t^{1/2}(\tau^{1/2} - t^{1/2})]^{-1} \tag{7.6.4}$$

and $(dE/dt)_{\text{min}}$ occurs at $t = \tau/4$ with the value

$$\left(\frac{dE}{dt}\right)_{\text{min,irrev}} = -\frac{2RT}{\alpha n_a F\tau} \tag{7.6.5}$$

Determination of τ by this approach is freer from problems of double-layer charging, because it is evaluated at a position in the curve before the transition time region where an appreciable charging current contribution exists. However, the large charging current contribution at the start of the chronopotentiogram still contributes. Even so, by using τ values evaluated from $(dE/dt)_{\text{min}}$ and applying the double-layer correction approach embodied in equation 7.3.19, extensions of chronopotentiometric measurements to low concentrations (e.g., 10^{-6} M Cd^{2+}) and very short times (e.g., τ values in the μsec region) are possible (15, 30, 31). This derivative approach does suffer from a need for knowledge about the degree of reversibility of the electrode reaction and, if it is irreversible, knowing the α value.

An alternate instrumental approach involves using the generated (dE/dt) value to produce a feedback signal representing i_c. This is then added to i applied to the cell to yield a more constant i_f (32). This approach requires a fair amount of instrumental complexity and is only partially successful, since a known and assumed constant value of C_d must be used to obtain i_c. Applications of this method, and chronopotentiometric techniques in general, to analytical or mechanistic problems have been rather sparse compared to the use of controlled potential techniques (27, 33, 34).

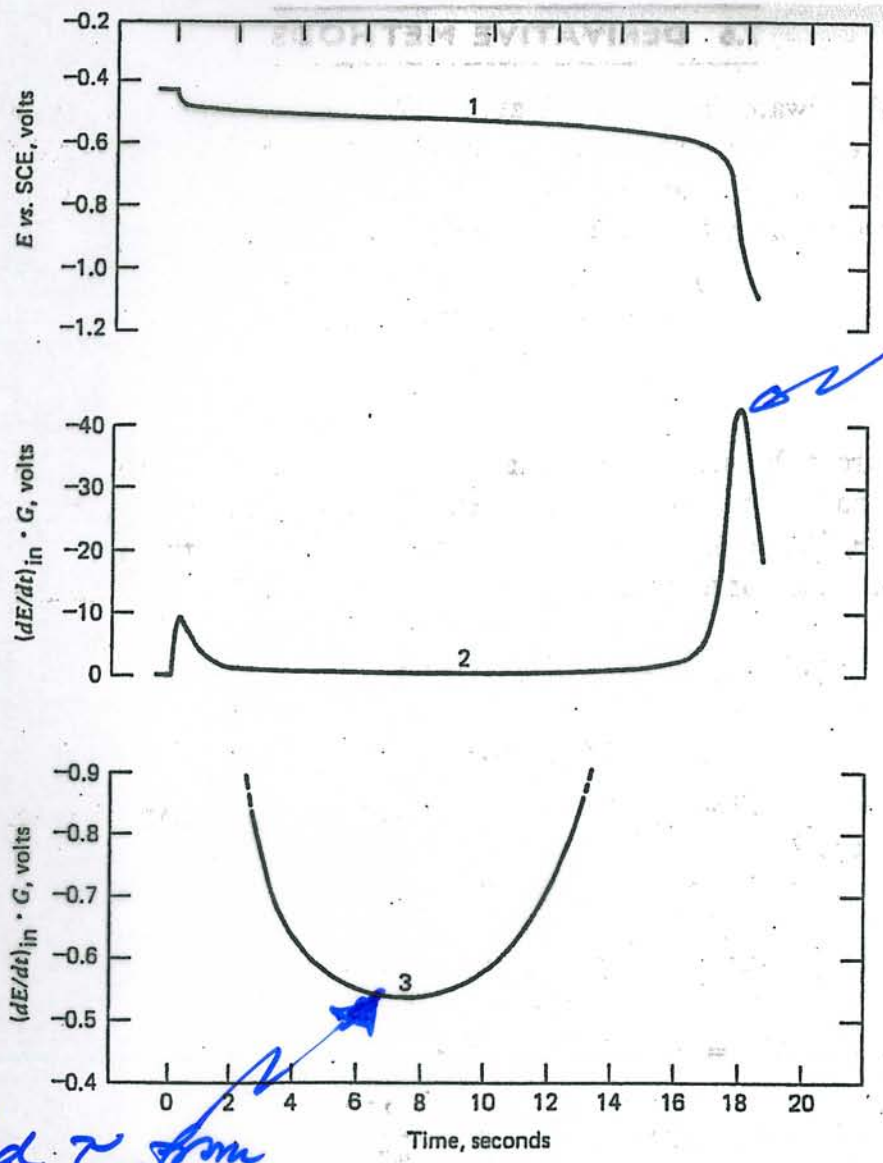

Figure 7.6.1

Experimental conventional and derivative chronopotentiograms. Reduction of 6.28 m*M* Tl(I) in 0.1 *M* KNO_3 at mercury pool cathode (1.38 cm^2 area) at $i = 0.503$ mA. Curve 1: Conventional *E-t* curve. Curve 2: Derivative curve, $(dE/dt)_{in} \cdot G$, represents the value of dE/dt (mV/sec) multiplied by gain in circuit, G (0.1095 V mV^{-1} sec). Curve 3: As in curve 2, with portion near region of minimum enlarged. [Reprinted with permission from D. G. Peters and S. L. Burden, *Anal. Chem.*, 38, 530 (1966). Copyright 1966, American Chemical Society.]

15. P. E. Sturrock, G. Privett, and A. R. Tarpley, *J. Electroanal. Chem.*, **14**, 303 (1967).

27. C. N. Reilley, G. W. Everett, and R. H. Johns, *Anal. Chem.*, **27**, 483 (1955).
28. H. B. Herman and A. J. Bard, *Anal. Chem.*, **36**, 971 (1964).
29. D. G. Peters and S. L. Burden, *Anal. Chem.*, **38**, 530 (1966).
30. P. E. Sturrock, J. L. Hughey, B. Vaudreuil, G. O'Brien, and R. H. Gibson, *J. Electrochem. Soc.*, **122**, 1195 (1975).
31. P. E. Sturrock and R. H. Gibson, *J. Electrochem. Soc.*, **123**, 629 (1976).
32. W. D. Shults, F. E. Haga, T. R. Mueller, and H. C. Jones, *Anal. Chem.*, **37**, 1415 (1965).
33. L. Gierst and A. Juliard, *Proc. Intern. Comm. Electrochem. Thermodynam. and Kinet.*, 2nd meeting, 1950, pp. 117, 279.
34. D. G. Davis, *Electroanal. Chem.*, **1**, 157 (1966).

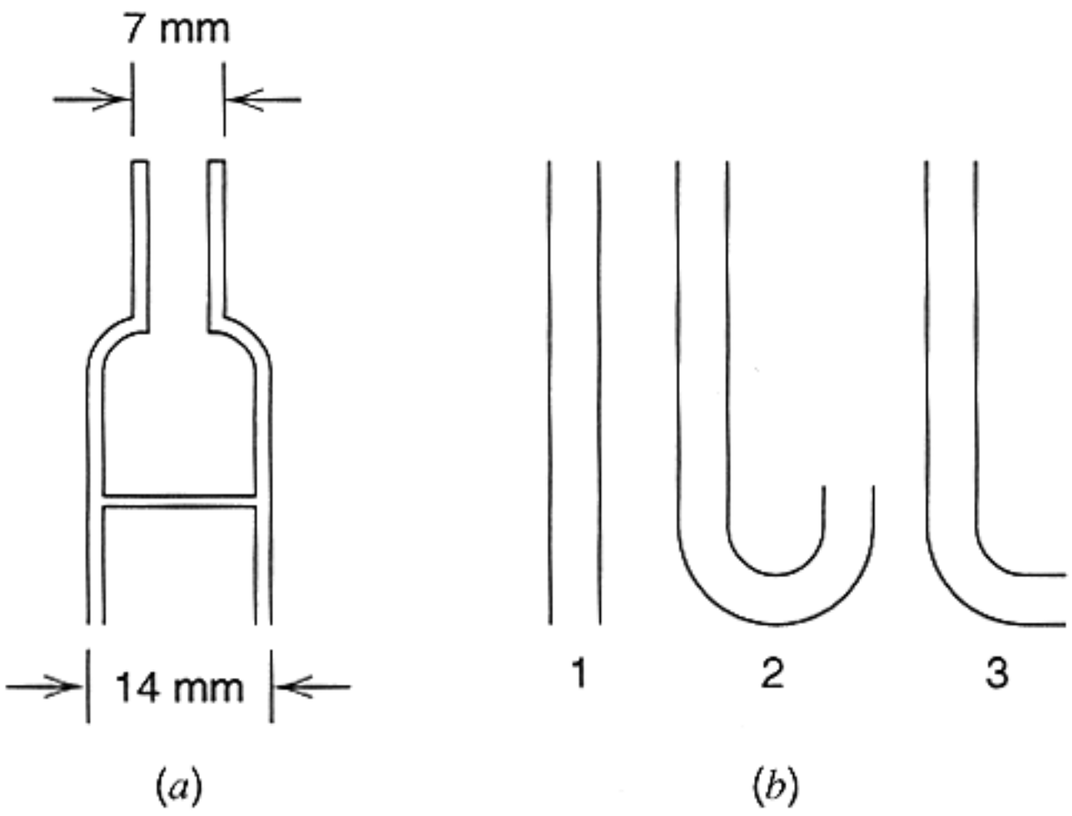

Figure 8.3.3 (*a*) Shielded electrode for maintaining linear diffusion and suppressing convection. (*b*) Tubes to which shielded electrode is attached to provide: (*1*) horizontal electrode, diffusion upward; (*2*) horizontal electrode, diffusion downward; (*3*) vertical electrode. [Reprinted with permission from A. J. Bard, *Anal. Chem.*, **33**, 11 (1961). Copyright 1961, American Chemical Society.]

The effect of double-layer charging is clearly most important at small τ values (see equation 8.3.20). Problems with distorted *E-t* curves and the difficulty of obtaining corrected τ values have discouraged the use of controlled-current methods as opposed to controlled-potential ones.

In both controlled-current and controlled-potential methods, problems develop at long experimental times because of the onset of convection and the nonlinearity of diffusion. Convective effects, caused by motion of the solution with respect to the electrode, can arise by accidental vibrations transmitted to the cell (e.g., by hood fans, vacuum pumps, passing traffic) or as a result of density gradients building up at the electrode surface because of differences in density between reactants and products (so-called "natural convection"). Convective effects can be minimized by using electrodes with glass mantles (shielded electrodes; Figure 8.3.3) and by orienting the electrode horizontally so that the denser species is always below the less dense one (15, 16). Vertically oriented electrodes (e.g., foils or wires) often suffer from convection effects even at not very long times (e.g., 60 to 80 s). The shielded electrode also has the virtue of constraining diffusion to lines normal to the electrode surface so that true linear diffusion conditions are approached. An unshielded electrode, such as a platinum disk imbedded in glass can show appreciable "sphericity" effects when the diffusion layer thickness is not negligible with respect to the electrode dimensions; that is, material can diffuse to the unshielded electrode from the sides. This effect causes increases in the transition time (or anomalously large currents in controlled-potential methods). With properly oriented shielded electrodes, however, linear diffusion conditions can be maintained for 300 s or longer.

▶ 8.4 REVERSAL TECHNIQUES

8.4.1 Response Function Principle

A useful technique for treating reversal methods in chronopotentiometry (and other techniques in electrochemistry) is based on the *response function principle* (2, 17). This method, which is also used to treat electrical circuits, considers the system's response to a perturbation or excitation signal, as applied in Laplace transform space. One can write the general equation (2)

$$\bar{R}(s) = \bar{\Psi}(s)\bar{S}(s) \tag{8.4.1}$$

where $\bar{\Psi}(s)$ is the excitation function transform, $\bar{R}(s)$ is the response transform, which describes how the system responds to the excitation, and $\bar{S}(s)$ is the system transform, which

connects the excitation and the response. For example for current excitation we can write, from (8.2.8) at $x = 0$,

$$\bar{C}_O(0, s) = C_O^*/s - [nFAD_O^{1/2}s^{1/2}]^{-1}\bar{i}(s) \tag{8.4.2}$$

or

$$\bar{C}_O^* - \bar{C}_O(0, s) = [nFAD_O^{1/2}s^{1/2}]^{-1}\bar{i}(s) \tag{8.4.3}$$

In this case $\bar{\Psi}(s) = \bar{i}(s)$ (the transform of the applied current perturbation), $\bar{R}(s) = \bar{C}_O^* - \bar{C}_O(0, s)$,the transform of the concentration response to the perturbation, and $\bar{S}(s) = [nFAD_O^{1/2}s^{1/2}]^{-1}$, which is characteristic of the system under excitation (semi-infinite linear diffusion). For controlled-current problems involving different systems (e.g., spherical or cylindrical diffusion, first-order kinetic complications) other system transforms would be employed.[2] We have illustrated how this equation could be employed for constant and programmed current methods, using appropriate $\bar{i}(s)$ functions. We now extend its use to reversal techniques.

8.4.2 Current Reversal (18, 19)

Consider a solution where only O is present initially at a concentration C_O^*, semi-infinite linear diffusion conditions prevail, and a constant cathodic current i is applied for a time t_1 (where $t_1 \leq \tau_1$, with τ_1 being the forward transition time). At t_1 the current is reversed, that is, the direction of the current is changed from cathodic to anodic, so that R formed during the forward step is oxidized to O, and the time τ_2 (measured from t_1) at which C_R at the electrode surface drops to zero is noted. At τ_2, the *reverse transition time*, the potential shows a rapid change toward positive values. We desire an expression for τ_2. This is most easily accomplished using the "zero shift theorem" of Section A.1.7. Since for $0 < t \leq t_1$, $i(t) = i$, and for $t_1 < t \leq t_1 + \tau_2$, $i(t) = -i$, the expression for the current, using step function notation, is

$$i(t) = i + S_{t_1}(t)(-2i) \tag{8.4.4}$$

so that the transform is given by

$$\bar{i}(s) = \frac{i}{s} - \frac{(2e^{-t_1 s})i}{s} = \left(\frac{i}{s}\right)(1 - 2\,e^{-t_1 s}) \tag{8.4.5}$$

Introducing this into (8.4.3), we obtain

$$\frac{C_O^*}{s} - \bar{C}_O(0, s) = \left(\frac{i}{s}\right)(1 - 2\,e^{-t_1 s})(nFAD_O^{1/2}s^{1/2})^{-1} \tag{8.4.6}$$

The analogous expression for $\bar{C}_R(0, s)$ [see (8.2.9)] is

$$\bar{C}_R(0, s) = \left(\frac{i}{s}\right)(1 - 2\,e^{-t_1 s})(nFAD_R^{1/2}s^{1/2})^{-1} \tag{8.4.7}$$

The inverse transform of (8.4.7) yields an expression for $C_R(0, t)$ at any time [recall that $S_{t_1}(t) = 0$ for $t \leq t_1$; $S_{t_1}(t) = 1$ for $t > t_1$; Section A.1.7]:

$$C_R(0, t) = \frac{2i}{nFA\pi^{1/2}D_R^{1/2}}[t^{1/2} - 2S_{t_1}(t)(t - t_1)^{1/2}] \tag{8.4.8}$$

At $t = t_1 + \tau_2$, $C_R(0, t) = 0$, so that $(t_1 + \tau_2)^{1/2} = 2\tau_2^{1/2}$ and

$$\boxed{\tau_2 = t_1/3} \qquad t_1 < \tau_1 \tag{8.4.9}$$

[2]This approach, and transform methods in general, are useful only for linear problems; hence second-order reactions or nonlinear complications cannot be treated by this technique.

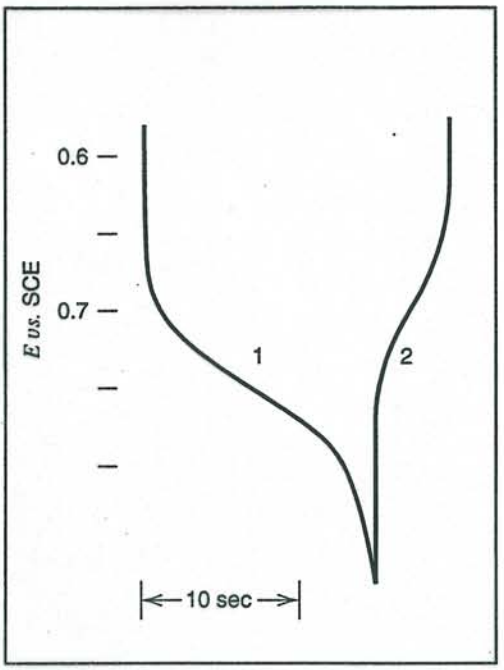

Figure 8.4.1 Typical experimental chronopotentiogram with current reversal. Oxidation of diphenylpicrylhydrazyl (DPPH) followed by reduction of the stable radical cation, $DPPH^{+\cdot}$. Solution was acetonitrile containing 1.04 m*M* DPPH and 0.1 *M* $NaClO_4$. The current was 100 μA, and a shielded platinum electrode of area 1.2 cm^2 was employed. [Reprinted with permission from E. Solon and A. J. Bard, *J. Am. Chem. Soc.*, **86**, 1926 (1964). Copyright 1964, American Chemical Society.]

Thus the reverse transition time (for stable R) is always 1/3 that of the forward time (Figure 8.4.1) up to and including τ_1, independent of D_O, D_R, C_O^*, and the rate of the electron transfer (assuming it is sufficiently rapid to show a reverse transition, that is, is not totally irreversible). The factor of 1/3 means that of the total amount of R generated during the forward step (equal to it_1/nF mol), only one-third returns to the electrode during the backward step up to τ_2, with the remainder diffusing into the bulk solution. At first thought, one might wonder at the independence of τ_2/t_1 on D_R. If D_R is very large, then a larger amount might be expected to diffuse away. However, a large D_R also implies that a larger amount will diffuse back during the reverse step, and the mathematics demonstrates that this exactly compensates for the diffusion away from the electrode. Thus the τ_2/t_1 ratio of 1/3 in chronopotentiometry is the analog of $i_r(2\tau)/i_f(\tau) = 0.293$ in potential step reversal (Section 5.7) and $i_{pc}/i_{pa} = 1.00$ in cyclic voltammetry (Section 6.5.1). Expressions can also be written for the potential-time behavior by combining the appropriate kinetic relationship with the equations for $C_O(0, t)$ and $C_R(0, t)$. For example, for a nernstian wave, $E_{0.215\tau_2} = E_{\tau/4}$. For a quasireversible system the separation between $E_{\tau/4}$ and $E_{0.215\tau_2}$ can be used to determine k^0 (20).

▶ 8.5 MULTICOMPONENT SYSTEMS AND MULTISTEP REACTIONS (19, 21–23)

Consider a solution containing two reducible substances, O_1 and O_2, at concentrations C_1^* and C_2^*, respectively, where the reduction $O_1 + n_1e \rightarrow R_1$ occurs first, and then, at more negative potentials, $O_2 + n_2e \rightarrow R_2$. Again, assuming semi-infinite linear diffusion, the following response-function equations can be written:

multicomponent

$$n_1FAD_1^{1/2}\left[\frac{C_1^*}{s} - \overline{C}_1(0, s)\right] = \frac{\overline{i}_1(s)}{s^{1/2}} \tag{8.5.1}$$

$$n_2FAD_2^{1/2}\left[\frac{C_2^*}{s} - \overline{C}_2(0, s)\right] = \frac{\overline{i}_2(s)}{s^{1/2}} \tag{8.5.2}$$

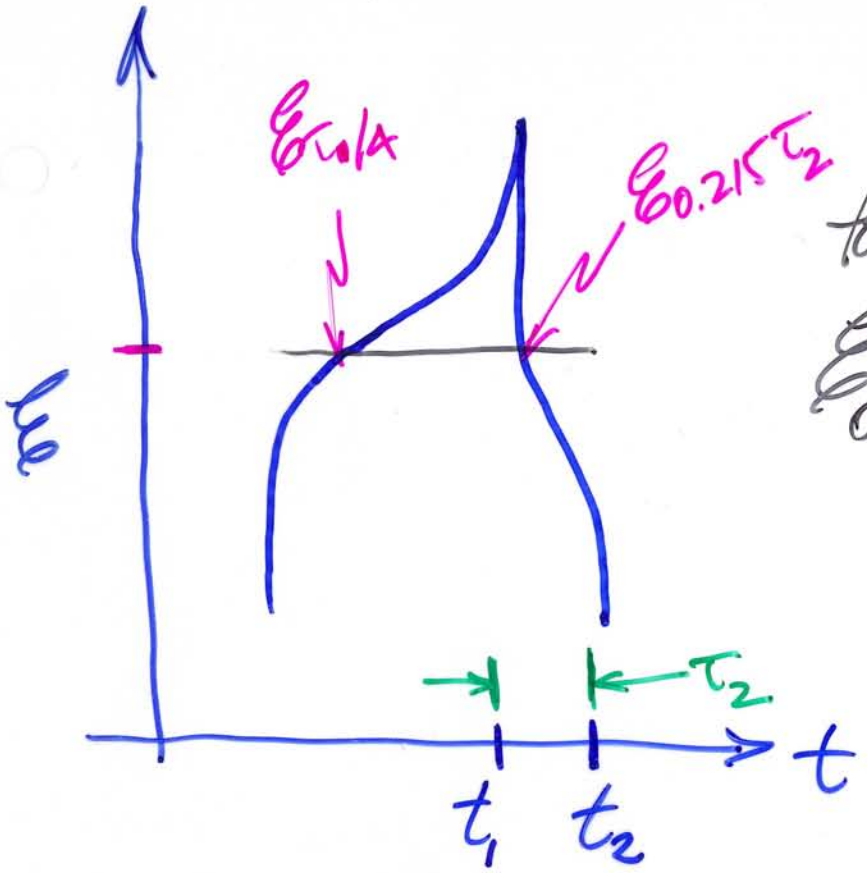

for Nernstian system

$$\mathcal{E}_{0.215\tau_2} = \mathcal{E}_{\tau_1/4}$$

"Shape of the Wave"

Tests

$$t_1 < \tau_1$$

$$t_2 - t_1 = \tau_2$$

where $\bar{i}_1(s)$ and $\bar{i}_2(s)$ are the transforms of the individual currents [$i_1(t)$ and $i_2(t)$] involved in the reduction of O_1 and O_2, respectively. Since the total applied current, $i(t)$, is $i_1(t) + i_2(t)$, then $\bar{i}(s) = \bar{i}_1(s) + \bar{i}_2(s)$, and from (8.5.1) and (8.5.2),

$$n_1 D_1^{1/2}\left[\frac{C_1^*}{s} - \bar{C}_1(0, s)\right] + n_2 D_2^{1/2}\left[\frac{C_2^*}{s} - \bar{C}_2(0, s)\right] = \frac{\bar{i}(s)}{FAs^{1/2}} \tag{8.5.3}$$

This equation is true at all times.

For the period when the potential is not sufficiently negative for O_2 reduction to occur (i.e., when $t \leq \tau_1$), $\bar{C}_2(0, s) = C_2^*/s$, $\bar{i}_2(s) = 0$, and (8.5.3) becomes identical to the simple equation (8.4.3), so that up to τ_1 the behavior is unaffected by the presence of O_2. For $t > \tau_1$, $\bar{C}_1(0, s) = 0$, so that (8.5.3) becomes

$$\frac{n_1 D_1^{1/2} C_1^*}{s} + n_2 D_2^{1/2}\left[\frac{C_2^*}{s} - \bar{C}_2(0, s)\right] = \frac{\bar{i}(s)}{FAs^{1/2}} \tag{8.5.4}$$

The second transition time ($t = \tau_1 + \tau_2$) occurs when the concentration of O_2 drops to zero at the electrode surface, that is, $\bar{C}_2(0, s) = 0$. Thus, for a constant current, $\bar{i}(s) = i/s$, and (8.5.4) for this time becomes

$$\frac{n_1 D_1^{1/2} C_1^*}{s} + \frac{n_2 D_2^{1/2} C_2^*}{s} = \frac{i}{FAs^{3/2}} \tag{8.5.5}$$

Inversion yields

$$(n_1 D_1^{1/2} C_1^* + n_2 D_2^{1/2} C_2^*)\left(\frac{FA\pi^{1/2}}{2}\right) = i(\tau_1 + \tau_2)^{1/2} \tag{8.5.6}$$

For example, for the special case $n_1 D_1^{1/2} C_1^* = n_2 D_2^{1/2} C_2^*$, $\tau_2 = 3\tau_1$. Thus, while in controlled-potential voltammetric methods two substances at equal concentration with equal diffusion coefficients show two waves of equal height, in chronopotentiometry unequal transition times arise. The long second transition results from the continued diffusion of O_1 to the electrode after τ_1, so that only a fraction of the applied current is available for reduction of O_2 (Figure 8.5.1).

Similar reasoning shows that for a stepwise process:

multistep

$$O + n_1 e \rightarrow R_1 \tag{8.5.7}$$

$$R_1 + n_2 e \rightarrow R_2 \tag{8.5.8}$$

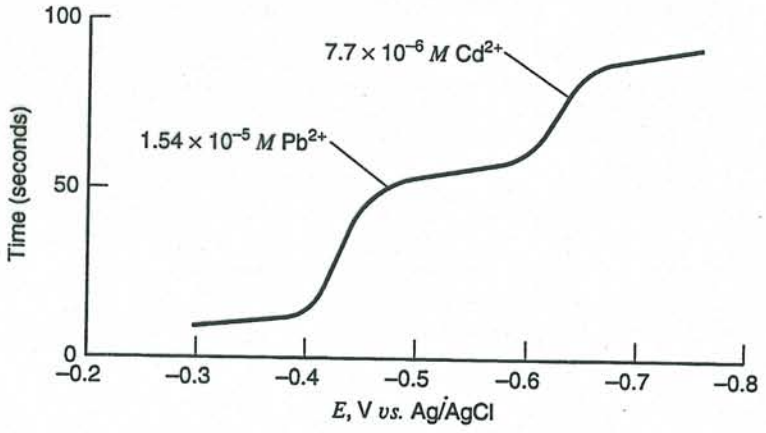

Figure 8.5.1 Consecutive reduction of Pb(II) and Cd(II) at a mercury pool electrode. Note that if *E-t* curve is plotted in this manner, it resembles a voltammogram. [Reprinted with permission from C. N. Reilley, G. W. Everett, and R. H. Johns, *Anal. Chem.*, **27**, 483 (1955). Copyright 1955, American Chemical Society.]

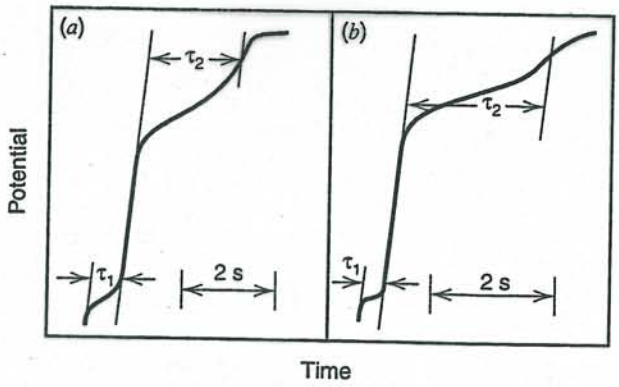

Figure 8.5.2 *E-t* curves for stepwise reduction of oxygen and uranyl ion at mercury electrode. (*a*) 1 *M* LiCl solution saturated with oxygen at 25°C. $O_2 + 2H_2O + 2e \rightarrow H_2O_2 + 2OH^-$; $H_2O_2 + 2e \rightarrow 2OH^-$; $\tau_2/\tau_1 \approx 3$. (*b*) 10^{-3} *M* uranyl nitrate in 0.1 *M* KCl + 0.01 *M* HCl. U(VI) + $e \rightarrow$ U(V); U(V) + $2e \rightarrow$ U(III); $\tau_2/\tau_1 \approx 8$. [Reprinted with permission from T. Berzins and P. Delahay, *J. Am. Chem. Soc.*, **75**, 4205 (1953). Copyright 1953, American Chemical Society.]

the transition time ratio is given by

$$\frac{\tau_2}{\tau_1} = \frac{2n_2}{n_1} + \left(\frac{n_2}{n_1}\right)^2 \tag{8.5.9}$$

Thus for $n_2 = n_1$, $\tau_2 = 3\tau_1$ (Figure 8.5.2). By use of the response-function principle one can show (Problem 8.4) that if a current of the form $i(t) = \beta t^{1/2}$ is used, then equal transition times result when $n_2 = n_1$.

8.6 THE GALVANOSTATIC DOUBLE PULSE METHOD

In Section 8.3.4, we saw that the single-pulse galvanostatic method cannot be used for fast electron-transfer reactions (i.e., those with large i_0), because the current is primarily nonfaradaic during the initial moments following the application of the current step, and it contributes mostly to charging C_d. Gerischer and Krause (24) developed a *galvanostatic double pulse method* (GDP), in which two constant-current pulses are applied to the electrode (Figure 8.6.1). The first (large) pulse I_1, applied for $0 < t < t_1$, mainly serves to charge the double layer to a potential that becomes the point of interrogation by a second, smaller pulse of current i_2. The basic idea is to use the short first pulse (typically 0.5 to 1 μs long) to drive the system to an overpotential that exactly supports the second current. Then η will not change when i_2 is applied, and there is no significant effect from charging the double layer during the second phase. A block diagram of apparatus for this technique is shown in Figure 8.6.2.

Some faradaic current does flow during the first pulse, and its effects must be taken into account. The theory of the GDP method was extended along that line by Matsuda, et al. (25). Valuable instrumental advances were later made by Aoyagi and coworkers (26–28).

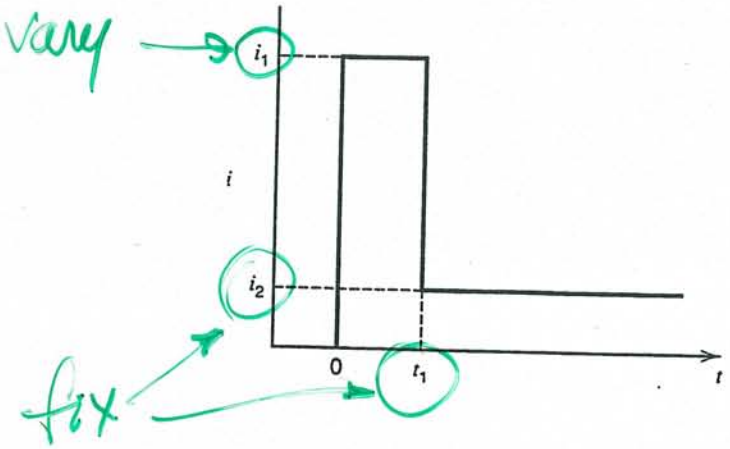

Figure 8.6.1 Excitation waveform for the galvanostatic double pulse method.

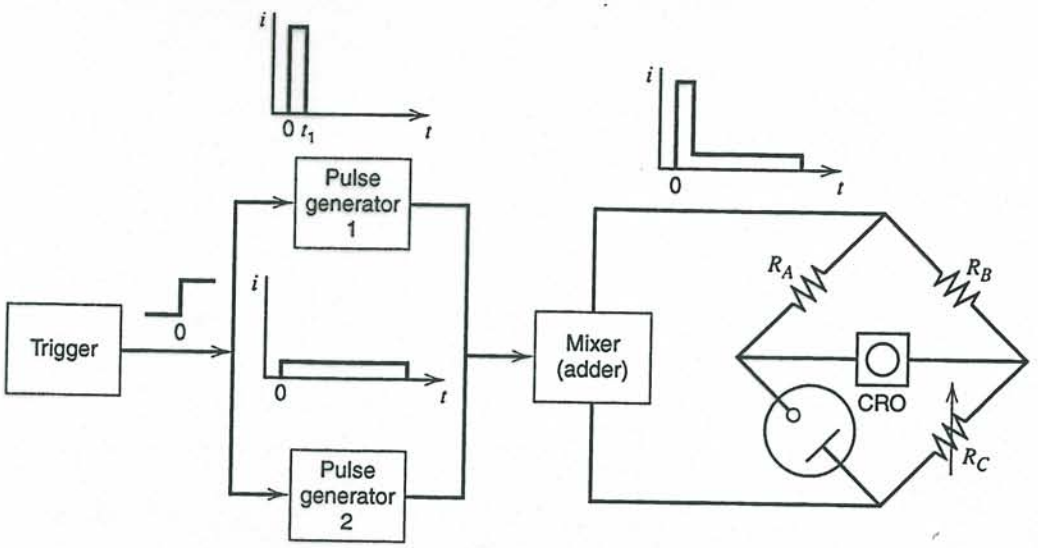

Figure 8.6.2 Block diagram for galvanostatic double-pulse method. A two-electrode cell (i.e., with a common counter/reference electrode) is placed in a bridge circuit for compensation of the cell ohmic resistance, R_Ω. The bridge is adjusted with $R_A = R_B$, $R_C = R_\Omega$, $R_A >> R_\Omega$ so that the pulse generators produce an essentially constant current through the cell. Provision is sometimes made in double pulse circuits, however, for a three-electrode cell and potentiostatic control of the working electrode before the application of the galvanostatic pulse. For details of such apparatus, see references 26–28.

When the ratio of pulse heights (i_1/i_2) is adjusted properly, and this is determined by trial and error, the *E-t* curve following the cessation of the first pulse is horizontal (Figure 8.6.3). Under these conditions, the overpotential for a quasireversible one-step, one-electron process is given by (25)

$$-\eta = \frac{RT}{F}\frac{i_2}{i_0}\left[1 + \frac{4Ni_0}{3\pi^{1/2}}t_1^{1/2} + \left(1 - \frac{9\pi}{32}\right)\left(\frac{4Ni_0}{3\pi^{1/2}}\right)^2 t_1 + \ldots\right] \qquad (8.6.1)$$

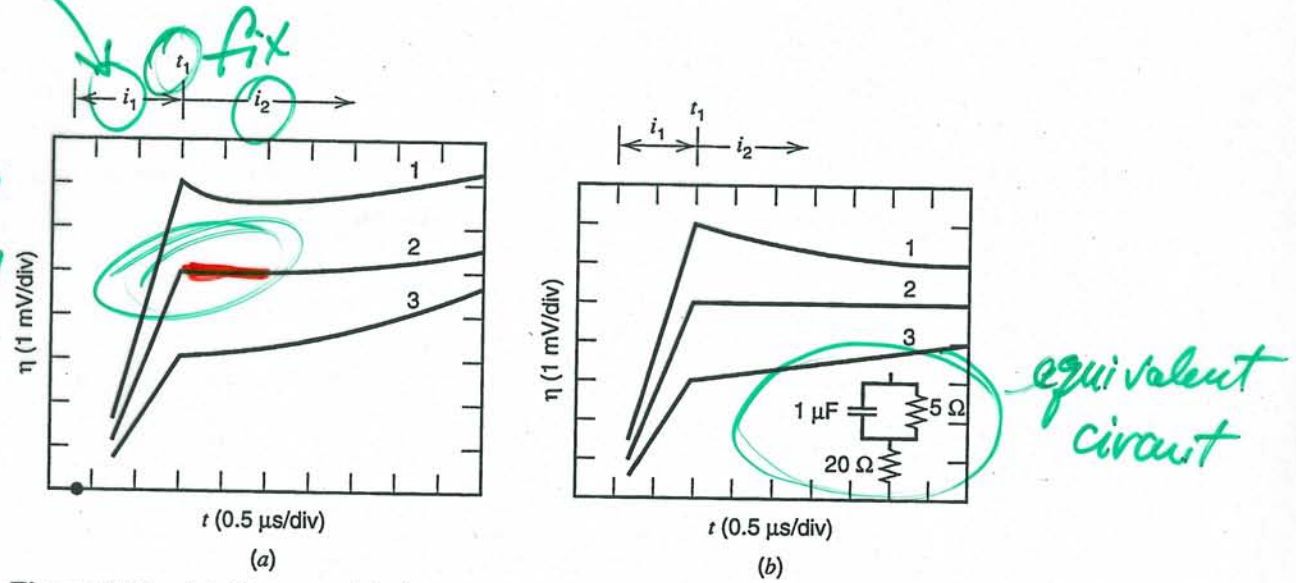

Figure 8.6.3 (*a*) Overpotential-time traces for galvanostatic double-pulse method for reduction of 0.25 m*M* Hg_2^{2+} in 1 *M* $HClO_4$ at an HMDE. Ratio i_2/i_1 was (*1*) 7.8, (*2*) 5.3, (*3*) 3.2; (*2*) shows the desired response for utilization of (8.6.2). (*b*) Voltage-time traces for constant-current double pulses applied to equivalent circuit shown. i_1 was (*1*) 7.6, (*2*) 5.5, (*3*) 3.3 mA; and i_2 = 1 mA. [From M. Kogoma, T. Nakayama, and S. Aoyagi, *J. Electroanal. Chem.*, **34**, 123 (1972), with permission.]

or, at sufficiently small values of t_1,

$$-\eta \approx \frac{RT}{F} i_2 \left(\frac{1}{i_0} + \frac{4N}{3\pi^{1/2}} t_1^{1/2} \right) \tag{8.6.2}$$

Thus one can carry out a series of experiments with different pulse widths t_1, and plot the value of η at the onset of i_2 *vs.* $t_1^{1/2}$ to obtain the exchange current from the intercept. Note the similarity between (8.3.10) and (8.6.2). The $t^{1/2}$ term in each case accounts for electrolytic modification of the surface concentrations. In the situation yielding (8.3.10), η was induced by current i; but in this case it is first induced by i_1 and then supported by i_2.

The differential double-layer capacitance can also be obtained from these data by the equation:

$$C_d = \lim_{t_1 \to 0} \frac{F t_1 i_0}{RTA} \left(\frac{i_1}{i_2} \right) \left(1 - \frac{4 N i_0 t_1^{1/2}}{3\pi^{1/2}} \right)^{-1} \tag{8.6.3}$$

This relation rests on the idea that the total charge in the first step, $i_1 t_1$, is purely nonfaradaic in the limit of very short t_1.

The GDP method does not require knowledge of the diffusion coefficients for reactant and products, or of the C_d value, for the calculation of i_0. Measurements using instrumentation developed by Aoyagi and coworkers suggest that rate constants of very rapid electrode reactions (~1 cm/s) can be determined using this technique.

▶ 8.7 CHARGE STEP (COULOSTATIC) METHODS

8.7.1 Principles

In the *charge-step* (or *coulostatic*) *method*, a very short-duration (e.g., 0.1 to 1 μs) current pulse is applied to the cell, and the variation of the electrode potential with time after the pulse (i.e., at open circuit) is recorded. The length of the current pulse is chosen to be sufficiently short that it causes only charging of the electrical double layer, so that even a very fast charge-transfer reaction does not proceed to an appreciable extent during this time. The pulse then serves only to inject a charge increment, Δq, and, in fact, under these conditions the method of charge injection or the actual shape of the injecting pulse (the coulostatic impulse) is unimportant. For example, the charge can be injected by discharging a small capacitor across the electrochemical cell (Figure 8.7.1) or with a pulse generator connected to the cell by a capacitor or switching diodes.

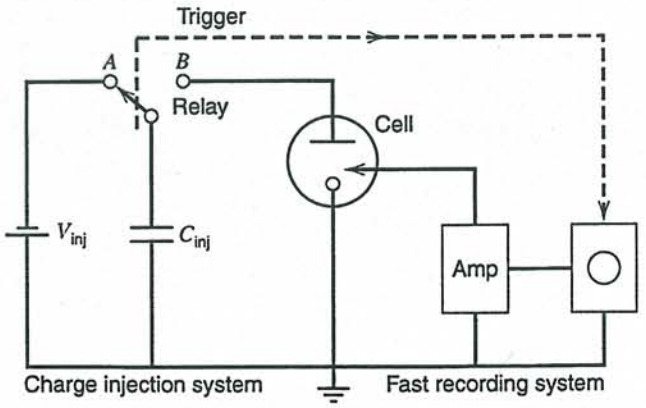

Figure 8.7.1 Circuit for charge-step or coulostatic method. In practice, the cell may be held initially at a potential E_{eq} by means of a potentiostat that is disconnected immediately before the charge injection.

For the circuit in Figure 8.7.1, when the relay is in position A, the capacitor, C_{inj}, is charged by the voltage source, V_{inj}, until the capacitor is charged by an amount

$$\Delta q = C_{inj} V_{inj} \tag{8.7.1}$$

For example, for $V_{inj} = 10$ V and $C_{inj} = 10^{-9}$ F, $\Delta q = 0.01\ \mu C$. When the relay switches to position B the charge is delivered to the electrochemical cell. Because the double-layer capacitance, C_d, is much larger than C_{inj}, essentially all of the charge will flow into the cell. The time required for this charge injection will depend on the cell resistance, R_Ω (Figure 8.7.2), with the time constant for injection being essentially $C_{inj}R_\Omega$ (Problem 8.6). This injected charge causes the potential of the electrode to deviate from its original value E_{eq} to a value $E(t = 0)$, where

$$E(t = 0) - E_{eq} = \eta(t = 0) = \frac{-\Delta q}{C_d} \tag{8.7.2}$$

The charge on C_d now discharges through the faradaic impedance (i.e., the heterogeneous electron-transfer process), and the open circuit potential moves back toward E_{eq} as $\eta(t)$ decreases to zero. Since the total external current i is zero, we have from (8.3.11) and (8.3.12),

$$i_f = -i_c = C_d\left(\frac{d\eta}{dt}\right) \tag{8.7.3}$$

or

$$\eta(t) = \eta(t = 0) + \frac{1}{C_d}\int_0^t i_f\, dt \tag{8.7.4}$$

Solution of (8.7.4) with the appropriate expression for i_f yields the desired expression for the variation of E (or η) with t. Note that if no faradaic reaction is possible at $E(t = 0)$ (i.e., at an ideally polarized electrode), C_d remains charged and the potential will not decay [i.e., for $i_f = 0$, $E = E_{eq} + \eta(t = 0)$ at all t].

We will now examine the E-t behavior following a coulostatic impulse for several cases of interest. Details of the theoretical treatments have been given by Delahay (29, 30) and Reinmuth (31, 32) and their coworkers, who first described the application of this technique.

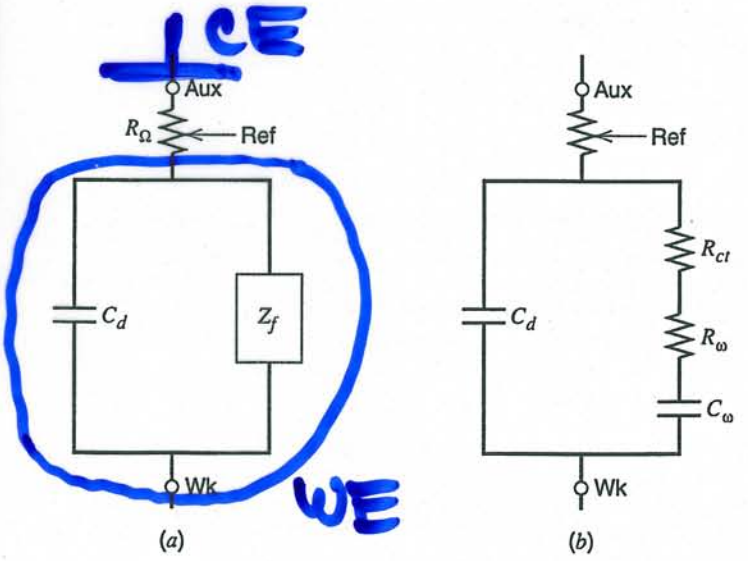

Figure 8.7.2 Equivalent circuit of cell with (*a*) R_Ω, the solution resistance, C_d, the double-layer capacitance, and Z_f, the faradaic impedance. The faradaic impedance represents the effect of the heterogeneous electron-transfer process. Often Z_f is broken down into the components shown in (*b*), where the charge-transfer resistance R_{ct} manifests the kinetics of heterogeneous charge transfer, and the components of the Warburg impedance, R_w and C_w, manifest diffusional mass transfer (see Section 10.1.3).

8.7.2 Small-Signal Analysis

When a chemically reversible, but kinetically sluggish, system is being investigated and the potential excursion is sufficiently small, that is, when $\eta(t = 0) << RT/nF$ and mass-transfer effects are absent, one can use the linearized i-η relation, (3.5.49),

$$-\eta = \frac{RT}{nFi_0} i \tag{8.7.5}$$

to describe i_f in (8.7.4). Thus,

$$\eta(t) = \eta(t = 0) - \frac{nFi_0}{RTC_d} \int_0^t \eta(t)dt \tag{8.7.6}$$

This equation can be solved readily by the Laplace transform method (Problem 8.7) to yield

$$\boxed{\eta(t) = \eta(t = 0) \exp\left(\frac{-t}{\tau_c}\right)} \tag{8.7.7}$$

$$\boxed{\tau_c = \frac{RTC_d}{nFi_0} = R_{ct}C_d} \tag{8.7.8}$$

Thus under these conditions, the potential relaxes exponentially toward E_{eq} with a time constant τ_c, governed by the rate of the charge-transfer reaction (Figure 8.7.3). This result can also be obtained from the equivalent circuit in Figure 8.7.2*b* by noting that R_w and C_w are negligible, so that C_d discharges only through the charge-transfer resistance R_{ct}, given by (3.5.50), with a time constant C_dR_{ct}. When (8.7.7) holds, a plot

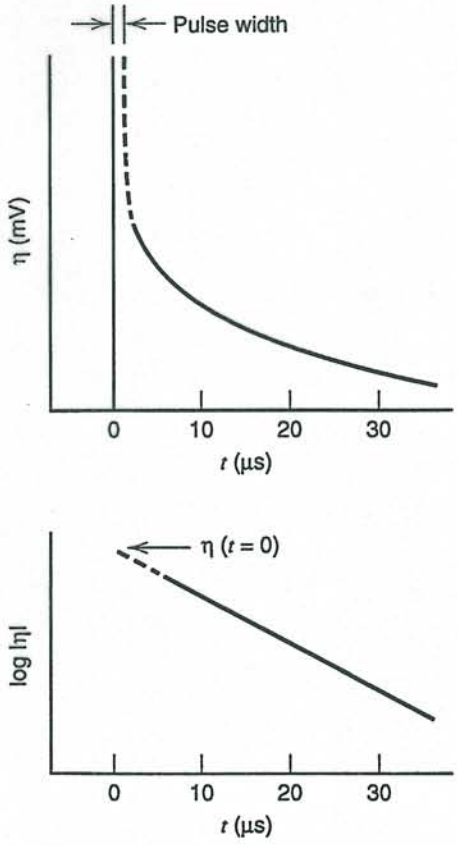

Figure 8.7.3 Typical coulostatic relaxation curves for a totally irreversible reaction.

of ln $|\eta|$ *vs.* t is linear with an intercept $|\eta(t = 0)|$ [which can be used to determine C_d by (8.7.2)] and a slope $-1/\tau_c$, which yields the charge-transfer resistance and the exchange current.

On the other hand, when R_{ct} is negligible compared to the mass-transfer impedance, which is the case for a nernstian system, the following expression applies:

$$\eta(t) = \eta(t = 0) \exp\left(\frac{t}{\tau_D}\right) \operatorname{erfc}\left[\left(\frac{t}{\tau_D}\right)^{1/2}\right] \tag{8.7.9}$$

$$\tau_D^{1/2} = \frac{RTC_d}{n^2F^2}\left(\frac{1}{C_O^* D_O^{1/2}} + \frac{1}{C_R^* D_R^{1/2}}\right) \tag{8.7.10}$$

The general small-signal expression for the case where both charge and mass-transfer terms are significant is (32)

$$\eta(t) = \frac{\eta(t = 0)}{\gamma - \beta}\left[\gamma \exp(\beta^2 t) \operatorname{erfc}(\beta t^{1/2}) - \beta \exp(\gamma^2 t) \operatorname{erfc}(\gamma t^{1/2})\right] \tag{8.7.11}$$

$$\beta, \gamma = \frac{\tau_D^{1/2}}{2\tau_c} \pm \frac{(\tau_D/4\tau_c) - 1]^{1/2}}{\tau_c^{1/2}} \tag{8.7.12}$$

(where the + is associated with β and the − with γ). Note that $\beta + \gamma = \tau_D^{1/2}/\tau_c$ and $\beta\gamma = 1/\tau_c$.

Clearly the analysis of experimental data for the determination of i_0 is easiest when (8.7.7) applies; this requires that $\tau_c >> \tau_D$. Detailed discussions of the analysis of coulostatic data and relaxation curves have appeared (33, 34).

8.7.3 Large Steps—Coulostatic Analysis

Consider the application of a charge step sufficiently large that the potential changes from E_{eq} to a value, $E(t = 0)$, corresponding to the diffusion plateau of the voltammetric wave. We assume that the double-layer capacity, C_d, is independent of potential in this region. The faradaic current that flows under these conditions at a planar electrode is given by (5.2.11). Introduction of this expression into (8.7.4) yields

$$E(t) = E(t = 0) + \left(\frac{nFAD_O^{1/2}C_O^*}{\pi^{1/2}C_d}\right)\int_0^t t^{-1/2}\,dt \tag{8.7.13}$$

$$\Delta E = E(t) - E(t = 0) = \frac{2nFAD_O^{1/2}C_O^* t^{1/2}}{\pi^{1/2}C_d} \tag{8.7.14}$$

The sign of ΔE is positive, since the electrode relaxes from a more negative initial potential toward more positive values. A plot of ΔE *vs.* $t^{1/2}$ is linear with a zero intercept and a slope $2nFAD_O^{1/2}C_O^*/(\pi^{1/2}C_d)$, which is proportional to the solution concentration (Figure 8.7.4).

This method has been suggested for the determination of small concentrations of electroactive materials (35, 36), but it has not been widely applied, probably because it requires recording of the E-t curve and is less readily automated than, for example, pulse voltammetry.